Repigmentation by combined narrow-band ultraviolet B/adipose-derived stem cell transplantation in the mouse model: Role of Nrf2/HO-1-mediated Ca^{2+} homeostasis

YUANYUAN BIAN[1*], HAO YU[2*], MINGZHU JIN[1] and XINGHUA GAO[1]

[1]Department of Dermatovenereal Disease, The First Affiliated Hospital of China Medical University, Shenyang, Liaoning 110001; [2]Department of Endocrinology, General Hospital of Northern Theater Command, Shenyang, Liaoning 110016, P.R. China

Received August 4, 2020; Accepted July 16, 2021

DOI: 10.3892/mmr.2021.12522

Abstract. Vitiligo is a depigmentation disease commonly seen in clinical practice, mainly involving loss of functional epidermal pigment cells and hair follicle melanocytes. Narrow-band ultraviolet B (NB-UVB) has emerged as the first choice of treatment for vitiligo, but long-term exposure may have serious consequences. Recently, it was reported that adipose-derived stem cells (ADSCs) improve melanocyte growth and the efficacy of melanocyte transplantation. The present study aimed to examine the efficacy of NB-UVB/ADSC-transplantation combined therapy on a mouse vitiligo model and explore the underlying mechanisms by focusing on endoplasmic reticulum stress and cellular calcium (Ca^{2+}) homeostasis. Vitiligo mice models were established by applying 40% monobenzone (MBZ) cream twice daily and treated with NB-UVB/ADSC combination therapy. Some treated mice were also given ML385, a nuclear factor erythroid 2 like 2 (Nr2) inhibitor. Histopathological changes were evaluated using a depigmentation evaluation score and observed with hematoxylin and eosin staining on skin tissues. ELISA was used to measure diagnostic markers in plasma. Flow cytometric assay was performed to quantify $CD3^+$, $CD4^+$ and $CD8^+$ levels. Expression levels of associated proteins were detected with western blot and immunofluorescence. Treatment of mice with MBZ-induced depigmentation patches on the skin was accompanied with loss of redox balance and disruption of cellular Ca^{2+} homeostasis. Oxidative stress and Ca^{2+} unbalancing were improved after the mice were treated by NB-UVB/ADSCs transplantation combination therapy. ML385, strongly negated the protective effect of NB-UVB/ADSC transplantation combination therapy, indicating the critical role of Nr2 signaling. The findings improved the understanding of the pathogenesis of vitiligo and will guide future development of therapeutic strategies against it.

Introduction

Vitiligo is a depigmentation disease commonly seen in clinical practice, mainly involving epidermal functional pigment cells and hair follicle melanocytes. The main clinical features are creamy white skin patches or flecks, often involving the head, face, neck, limbs and other parts of the body (1). It has a prevalence of ~1-2% worldwide (2). Vitiligo has a serious impact on the life of patients (3).

Accumulating evidence suggests that oxidative stress serves a critical role in vitiligo (4). For example, oxidative stress reportedly enhances the secretion of inducible heat-shock protein 70 in the skin, which leads to melanocyte loss (5). Antioxidant enzymes such as superoxide dismutase (SOD) and glutathione peroxidase are present in high levels in tissue from patients with vitiligo (6). Severe oxidative stress extends to the endoplasmic reticulum (ER), resulting in ER stress through the accumulation of misfolded proteins and structural aberration, which then lead to melanocyte destruction *in vivo* (7). Disruption of ER redox balance disturbs cellular calcium (Ca^{2+}) homeostasis, which in turn activates ER stress and triggers apoptosis (8).

A previous study demonstrated that the inhibition of oxidative stress could be an effective therapy for vitiligo (6). Phototherapy remains the primary vitiligo treatment; using ultraviolet (UV) lamps or lasers, phototherapy helps ameliorate vitiligo through immunosuppression and stimulation of melanocyte generation (9). The narrow-band (NB)-UVB, a subset of type B ultraviolet light, has emerged as one of the most effective and the safest therapies even for pregnant women and children and it is presently the first choice for clinical treatment of vitiligo (10). However, long-term treatment with NB-UVB risks damaging the skin (11,12).

Correspondence to: Dr Xinghua Gao, Department of Dermatovenereal Disease, The First Affiliated Hospital of China Medical University, 155 Nanjingbei Street, Heping, Shenyang, Liaoning 110001, P.R. China
E-mail: gaobarry@hotmail.com

*Contributed equally

Key words: vitiligo, adipose-derived stem cells, narrow-band ultraviolet B, endoplasmic reticulum stress, calcium homeostasis, nuclear factor erythroid 2 like 2 signaling

Adipose-derived stem cells (ADSCs) are a subset of mesenchymal stem cells with similar properties, such as regeneration and differentiation into various cell lineages (13). Since ADSCs are ubiquitous and abundant in subcutaneous adipose tissues and can be obtained easily, ADSCs-based therapies were clinically applied in numerous diseases during the last decade (14). ADSCs were used directly for damaged tissue recovery through the secretion of wound healing-related growth factors (15). The capacity of ADSCs to differentiate into osteoblasts and chondroblasts was widely applied for clinical cases of bone regeneration (16). Importantly, ADSCs can improve melanocyte growth *in vitro* and the efficacy of melanocyte transplantation *in vivo* (17). These findings provide new insights into future development of therapeutic strategies against vitiligo.

The present study examined the efficacy of a combination therapy of NB-UVB and ADSCs transplantation on monobenzone (MBZ)-induced vitiligo in mice. In addition, ER stress and Ca^{2+} homeostasis were examined to identify their possible role in melanocyte survival and proliferation.

Materials and methods

Vitiligo model. Four-week-old female C57BL/6 mice (20-25 g) were purchased from the Department of Laboratory Animals, China Medical University (CMU). To minimize potential confounders, only females were recruited. All procedures were carried out according to Center for Animal Resources and Development regulations for animal care and approved by Institutional Animal Care and Use Committee (IACUC) of CMU (IACUC no. CMU2019211). The 40 mice were housed at room temperature (22-26˚C), 40-50% relative humidity with 12-h light/dark cycle and free access food and water. The condition of these mice was observed every day. Mice were divided into several groups using a random number table: Control group (Con, n=10), Vitiligo model group (VIT; n=10), vitiligo model treated with NB-UVB/ADSCs group (NUA; n=10) and vitiligo model treated with NB-UVB/ADSCs and Nrf2 Inhibitor ML385 (30 mg/kg; cat. no. SML1833; Sigma-Aldrich; Merck KGaA) group (NUAM; n=10). Authors were aware of group allocation at the different stages of the experiment. The sample size was decided upon by using data from previous similar studies (18,19). To prepare the vitiligo mice model, 40% monobenzone cream (Galan Pharmacy) was massaged twice a day for 50 days using a spatula on a 2x2 cm^2 shaved area on the backs of the mice. All mice were successfully prepared for the animal model and there were no exclusions. The mice in the Con group were treated with 50 ml vaseline. Whole blood was collected from the mice and allowed to clot undisturbed at room temperature in the absence or presence of heparin (Sigma-Aldrich; Merck KGaA) and the serum and plasma respectively were collected by centrifugation (2,000 x g, 20 min) at 4˚C. For molecular analysis, tissues from the perilesional skin of vitiligo lesions and healthy skin were homogenized using a RIPA lysis and extraction buffer (Thermo Fisher Scientific, Inc.). The procedure is shown in Fig. S1.

ADSCs isolation. ADSCs were isolated from the adipose tissues in the inguinal fat pads of mice at the beginning of the animal experiments (20). The adipose tissue was aseptically collected from the inguinal fat pads of the mice under anesthesia (2% 40 mg/kg pentobarbital sodium intraperitoneal injection). Fat pad tissues were excised, finely minced, then the adipose tissues were washed with phosphate-buffered saline (PBS; pH 7.4), followed by enzymatic digestion of tissues using 0.1% collagenase type I (Thermo Fisher Scientific, Inc.) for 1 h at 37˚C. After washing, the cellular pellet was isolated by centrifugation at 500 x g for 10 min at room temperature and further cultured in Dulbecco's modified Eagle's medium (DMEM, FUJIFILM Wako Pure Chemical Corporation) supplemented with 10% heat-inactivated fetal bovine serum (FBS; MP Biomedicals, LLC) and 1% penicillin-streptomycin (Nacalai Tesque, Inc.) in a 5% CO_2 humidified incubator at 37˚C.

ADSCs transplantation. Prior to transplantation, the hair of the mice was removed using an electric shaver. ADSCs were suspended at a density of $1x10^6$ cells/100 μl PBS and 100 μl of cell suspension were subcutaneously injected into the NUA and NUAM group mice with an insulin syringe. The needle was removed once the ADSCs suspension was completely absorbed. The mice in Con and VIT group were injected with 100 μl PBS (21).

NB-UVB irradiation. Mice were irradiated using a Therapie-systeme UV109B (Waldmann Group) with a spectrum range 310-315 nm and a maximum wavelength of 311 nm. NB-UVB therapy was given three times per week with an initial dose of 0.4 J/cm^2, independent of the skin type. The dose was increased by 0.05-0.1 J/cm^2 and the optimal constant dose was fixed when minimal erythema occurred in the lesions.

Nuclear factor erythroid 2 like 2 (Nrf2) inhibition. To understand the role of Nrf2/heme oxygenase 1 signaling in vitiligo, the ability of the classical Nrf2 inhibitor ML385 to affect NB-UVB/ADSCs transplantation treatment was examined as previously described (22). Briefly, ML385 was dissolved in DMSO firstly and then diluted it into 5% DMSO solution with PBS before being used. 30 mg/kg ML385 was administered intraperitoneally 1 h before NB-UVB/ADSCs treatment (23).

Depigmentation evaluation. The extent of depigmentation was objectively quantified and evaluated in the 1.5 cm^2 treated area by three observers for the 30 days of skin treatment and another 20 days afterwards. The depigmentation score of each mouse was recorded according to the Vitiligo Area Scoring Index (VASI) (24). The mouse is separated into four regions including head/neck, trunk, limbs (including axillary, inguinal and buttocks regions) and tail. Skin depigmentation in each region is classified into six percentage groups (0%, 0-10%, 10-25%, 25-50%, 50-75% and 75-100%) and scored from 0 to 5 as in Table I. Mice were evaluated on a visual scale and the highest score a mouse could achieve was 20. The depigmentation score of each group was the sum of independent scores of the mice in the corresponding experimental group.

Hematoxylin and eosin (HE) staining. Following the whole animal experiment, mice were euthanized by dislocating their cervical spine and death was verified by the cessation

Table I. Depigmentation evaluation score.

Score	0 (%)	1 (%)	2 (%)	3 (%)	4 (%)	5 (%)
Head/neck	0	0-10	10-25	25-50	50-75	75-100
Trunk	0	0-10	10-25	25-50	50-75	75-100
Limbs	0	0-10	10-25	25-50	50-75	75-100
Tail	0	0-10	10-25	25-50	50-75	75-100

of cardiovascular and respiratory activity. Skin tissue samples were fixed with 4% polyformaldehyde overnight at 4˚C., then the samples were dehydrated with gradient ethanol (v/v) 70, 80, 90 and 100% for 20 mins each. The samples were cleared with two changes of xylene, embedded in paraffin and sectioned at 5 μm for HE staining. Hematoxylin and eosin at room temperature were applied onto the sliced sections in turn for 4 min each. Histopathological changes were observed using a light microscope at x40 magnification and ≥5 randomly chosen fields.

ELISA. The diagnostic markers of vitiligo [tyrosinase (TYR), macrophage migration inhibitory factor (MIF) and monoamine oxidase (MAO)] were quantified using Mouse Tyrosinase ELISA kit (cat. no. MBS763418; MyBioSource, Inc.), Mouse MIF ELISA kit (cat. no. ab209885; Abcam) and Mouse monoamine oxidase ELISA kit (cat. no. MBS731375; MyBioSource, Inc.) respectively according to manufacturer's instructions. Additionally, Cu/Zn superoxide dismutase ELISA kit (cat. no. QIA97; Merck Millipore), MDA Assay Kit (cat. no. ab238537; Abcam). and Mouse MPO ELISA kit (cat. no. ab155458; Abcam) were correspondingly used to measure superoxide dismutase (SOD), malondialdehyde (MDA) and myeloperoxidase (MPO) in serum based on competitive binding between antibodies.

Flow cytometric analysis. The peripheral blood from mice was depleted of red blood cells by ammonium chloride buffering (Sigma-Aldrich; Merck KGaA). Cells were diluted to 1x10^5 cells/100 μl. Each sample was incubated with anti-CD16/32 (1:50; cat. no. 612783; BD Biosciences) monoclonal antibody at 4˚C for 20 min. Then cells were incubated with of FITC-CD3 (cat. no. 11-0032-82), FITC-CD4 (cat. no. MA5-17451) and FITC-CD8 antibodies (cat. no. MA1-10303; all Thermo Fisher Scientific, Inc.) at 4˚C for 20 min. After washing with PBS, cells were stained with 7-AAD (1:20; BD Biosciences; cat. no. 559925) for 15 min to exclude dead cells from analysis. Stained cells were analyzed using a FACSVerse flow cytometer (BD Biosciences) and FlowJo 7.6 software (FlowJo LLC). The CD4/CD8 ratio was calculated as follows: Number of $CD4^+$ cells/number of $CD8^+$ cells.

Western blotting. Calcium influx is a key factor in activating the ER stress response. To explore the involvement of Ca^{2+} homeostasis, western blotting was used to analyze the relevant proteins. Tissues were homogenized using a RIPA lysis and extraction buffer (Thermo Scientific, Inc.), followed concentration determination with a BCA Protein Assay kit (FUJIFILM Wako Pure Chemical Corporation). Proteins (20 μg) from each sample were separated by 7.5% acrylamide gel and transferred to polyvinylidene difluoride membranes overnight at 4˚C with a low voltage. After 5% skimmed milk was used to block membranes at room temperature for 1 h, the membrane was rinsed with TBS containing 0.1% Tween-20 (TBST) and incubated with primary antibodies (all Cell Signaling Technology, Inc.) against sarco-ER Ca^{2+} ATPase type2 (SERCA2; 1:1,000; cat. no. 9580), glucose-regulated protein (GRP) 75 (1:1,000; cat. no. 3593), GRP78 (1:1,000; cat. no. 3177), caspase-12 (1:1,000; cat. no. 2202), ryanodine receptor (RYR1; 1:1,000; cat. no. 8153), inositol 1,4,5-trisphosphate receptor (IP3R; 1:1,000; cat. no. 8568), voltage dependent anion channel 2 (VDAC2; 1:1,000; cat. no. 9412), mitochondrial calcium uniporter regulator 1 (MCUR1; 1:1,000; cat. no. 13706), Nrf2 (1:1,000; cat. no. 12721), HO-1 (1:1,000; cat. no. 86806) and Trx1 (1:1,000; cat. no. 2298) overnight at 4˚C. GAPDH (1:1,000; cat. no. 5174) was used as an internal control. Horseradish peroxidase-conjugated secondary anti-rabbit (cat. no. 5127) and anti-mouse antibody (both 1:5,000; cat. no. 70765; both Cell Signaling Technology, Inc.) were incubated at room temperature for 1 h. Protein band intensity was analyzed using Luminata Forte Western HRP Substrate (EMD Millipore) with a Bio-Rad ChemiDox XRS^+ imaging system (Bio-Rad Laboratories, Inc.) and ImageLab software (version 4.1, Bio-Rad).

Immunofluorescence. Immunofluorescence was used to measure ROS level in skin tissue using a commercial kit (Nanjing Jiancheng Bioengineering Institute). Mice was scarified after experiment. Mice skin lesion tissues were collected and snap-frozen in liquid nitrogen. Then skin tissues were sliced at 4 μm thickness. Sections were blocked in phosphate-buffered saline (PBS) with 2.5% goat serum (Thermo Fisher Scientific, Inc.) for 30 min at room temperature. Sections were incubated with 2,7-dichlorofluorescin diacetate (20 μM) at 37˚C for 60 min in the dark and washed three times with PBS. A total of five randomly selected fields from each tissue section were observed under a fluorescence microscope (Olympus Corporation; cat. no. IX71). The fluorescence intensity of ROS staining (x200 magnification) was analyzed using Image-Pro Plus 6.0 software (Media Cybernetics, Inc.).

Statistical analysis. One-way ANOVA followed by Bonferroni's multiple comparisons test was used to compare normalized protein levels from western blots of specific proteins in mice tissue. A non-parametric Kruskal-Wallis test followed by Dunn's multiple comparisons test was used to compare the results of depigmentation score, the levels of TYR, MIF,

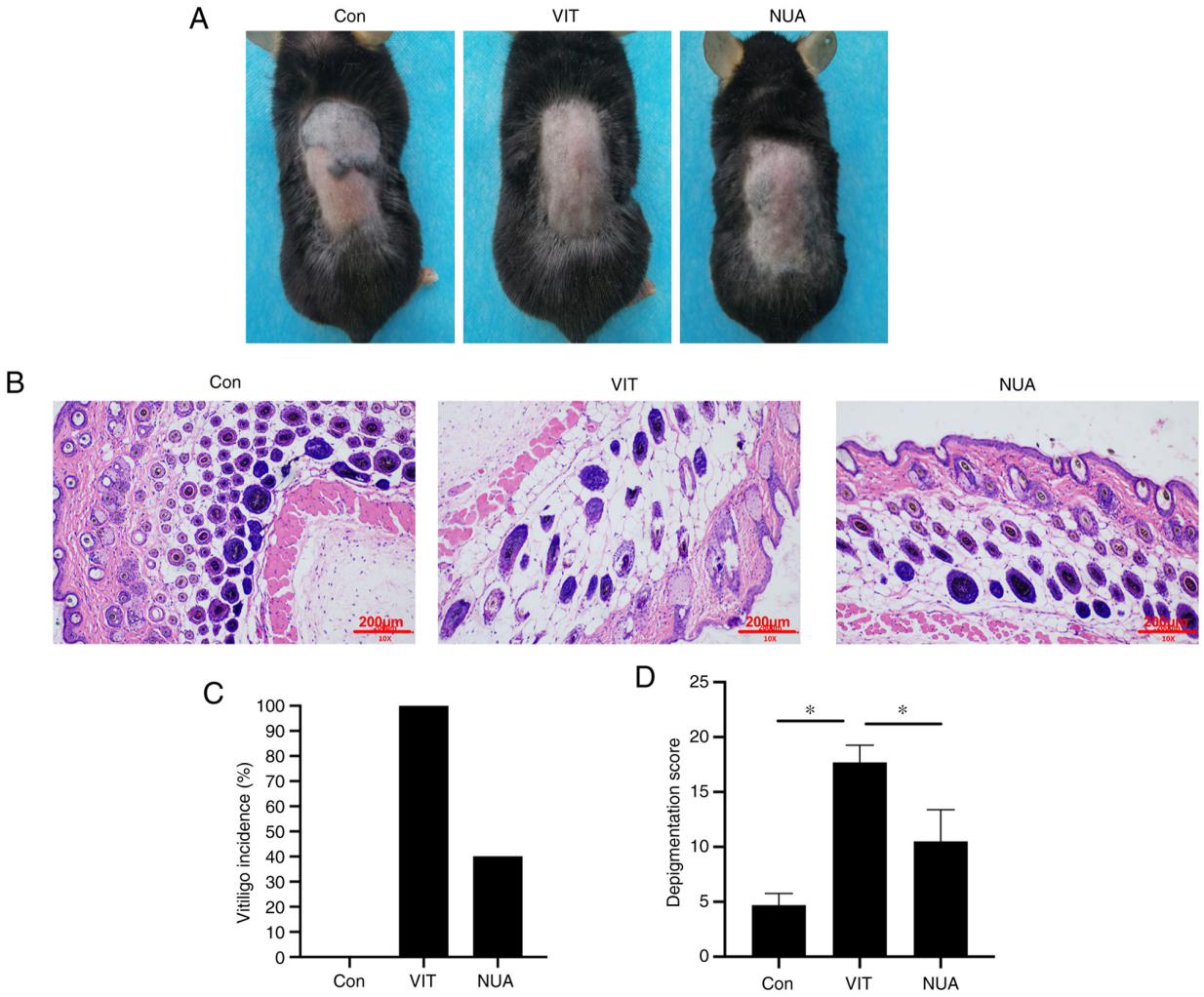

Figure 1. The protective effect of NB-UVB on ADSCs-transplanted vitiligo mice. (A) No white patches in mice were developed by Vaseline exposure. Vitiligo was developed with 40% monobenzone exposure. Vitiligo was rescued by NB-UVB/ADSCs application. (B) Hematoxylin and eosin staining to observe histopathological changes (scale bar=200 μm). (C) Vitiligo incidence and (D) depigmentation score level. The data are represented as the mean ± standard deviation (n=10). *P<0.05. NB-UVB, narrow band ultraviolet B; ADSCs, adipose-derived stem cells; Con, mice were treated with Vaseline only; VIT, mice in vitiligo model group treated with 40% monobenzone cream; NUA, mice treated with NB-UVB and ADSCs together.

MAO, MDA, MPO, SOD and the results of flow cytometry. Two-group comparisons were conducted by unpaired t-test. Data were represented as mean ± standard deviation using GraphPad Prism 5.0 (GraphPad Software, Inc.). P<0.05 was considered to indicate a statistically significant difference.

Results

The protective effect of NB-UVB and ADSCs-transplantation on vitiligo mice. To establish the vitiligo mice model, mice were topically treated with 40% MBZ. As shown in Fig. 1A, white patches were observed in MBZ-exposed areas, but not in the Con group. Following treatment with NB-UVB/ADSCs, white patches were significantly reduced. Significant histopathological changes were observed in skin tissues of mice in VIT group compared to mice in the Con group; namely dilated intercellular spaces, occurrence of cellular infiltration and acanthosis (Fig. 1B). Vitiligo incidence was also examined in the present study and it was found that the white patches occurred in ~100% of the MBZ-exposed mice (Fig. 1C) and the depigmentation score was remarkably elevated in contrast to mice in the Con group (Fig. 1D). In NUA mice, vitiligo incidence and the depigmentation score were markedly decreased.

Pathological changes in NB-UVB on ADSCs-transplanted vitiligo mice. Combination NB-UVB/ADSC transplantation treatment significantly reduced TYR concentrations in serum and increased MIF and MAO concentrations, while increasing TYR and reducing MIF and MAO concentrations in serum (Fig. 2A). Following treatment, the percentage of $CD3^+$ cells was increased significantly and the ratio of $CD4^+/CD8^+$ was reduced in peripheral blood in NUA group compared to the VIT group (Fig. 2B), suggesting that NB-UVB/ADSCs transplantation treatment could relieve the injury in the vitiligo mice model.

ER stress homeostasis is regulated by NB-UVB/ADSCs transplantation treatment. MDA and MPO levels increased and SOD decreased in MBZ-treated mice (Fig. 3A), indicating an imbalanced redox environment. Compared with untreated VIT mice, NB-UVB/ADSCs transplantation treatment increased SOD and reduced MDA and MPO in serum, indicating an

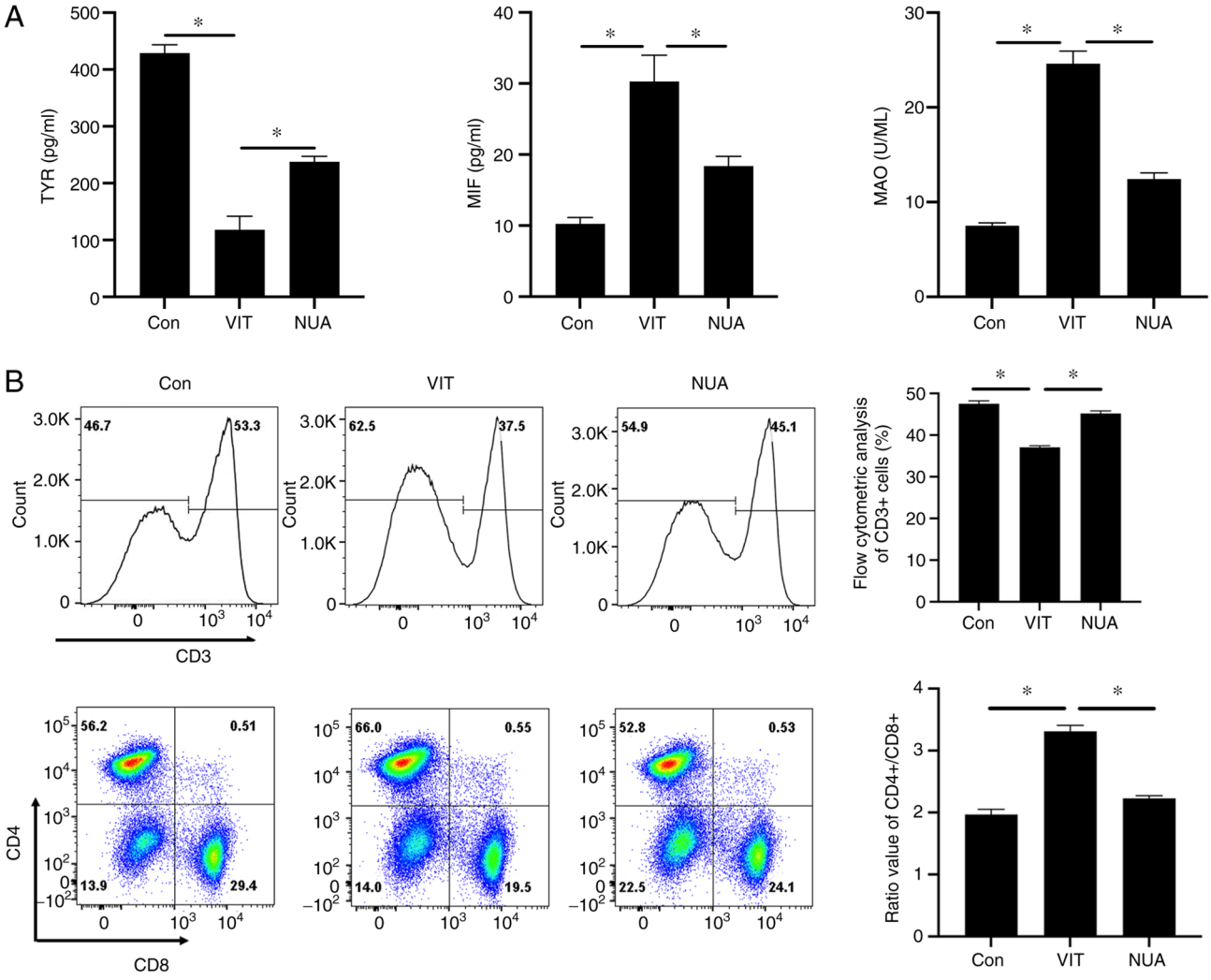

Figure 2. The pathological analysis of MBZ-exposed mice. (A) The diagnostic markers of vitiligo in serum were quantified by ELISA. (B) The subtypes of T cell were identified using flow cytometry. All the data are represented as the mean ± standard deviation (n=3). *P<0.05. MBZ, monobenzone; Con, mice were treated with Vaseline only; VIT, mice in vitiligo model group treated with 40% monobenzone cream; NUA, mice treated with narrow band ultraviolet B and adipose-derived stem cells together.

improvement in cellular oxidative stress (Fig. 3A). Increased ROS are an important signal of oxidative stress injury and combination treatment reduced ROS in mouse back skin (Fig. 3B). ER-stress indicators, including GRP78 and caspase-12, increased with MBZ exposure (Fig. 3C) along with GRP75 (Fig. 3D), an indicator of ER-mitochondrial coupling, suggesting crosstalk between the ER and mitochondria. ER stress imbalance was suppressed with NB-UVB/ADSCs transplantation treatment, which reduced levels of these stress indicator proteins (Fig. 3C and D).

Ca^{2+} homeostasis is regulated by NB-UVB/ADSCs transplantation treatment. Expression of SERCA2, an ER-localized calcium transporter, decreased after MBZ treatment, while expression of RYR1 and IP3R, two ER-localized Ca^{2+} release channels, increased (Fig. 4A). Expression of two mitochondria-located Ca^{2+} channels, VDAC2 and MCUR1, also increased with MBZ treatment (Fig. 4B). When the mice received NB-UVB/ADSCs transplantation treatment, these changes were reversed, suggesting Ca^{2+} overload was suppressed (Fig. 4).

NB-UVB/ADSCs treat vitiligo through modulating Nrf2/HO-1. As shown in Fig. 5A, ML385 successfully blocked Nrf2 signaling and MBZ treatment reduced expression of Nrf2 and suppressed its downstream signaling, including heme oxygenase 1 (HO-1) and thioredoxin (Trx1). Expression of Ca^{2+} channels including RYR1, IP3R, VDAC2 and MCUR1 increased in NB-UVB/ADSCs transplantation-treated vitiligo mice after Nrf2 inhibitor treatment (Fig. 5B). Additionally, inhibition of ER stress-related proteins by NB-UVB/ADSCs transplantation was cancelled following Nrf2 inhibitor treatment (Fig. 5C). Diagnostic markers of vitiligo in ML385-treated mice were similar to those of MBZ-treated mice (Fig. 5D).

Discussion

The present study demonstrated that depigmentation patches occurred in both drug-exposed locations and non-exposed locations when the mice were treated with 40% MBZ. Changes in the diagnostic markers of vitiligo and anti-oxidative enzymes suggested that the mouse model of vitiligo

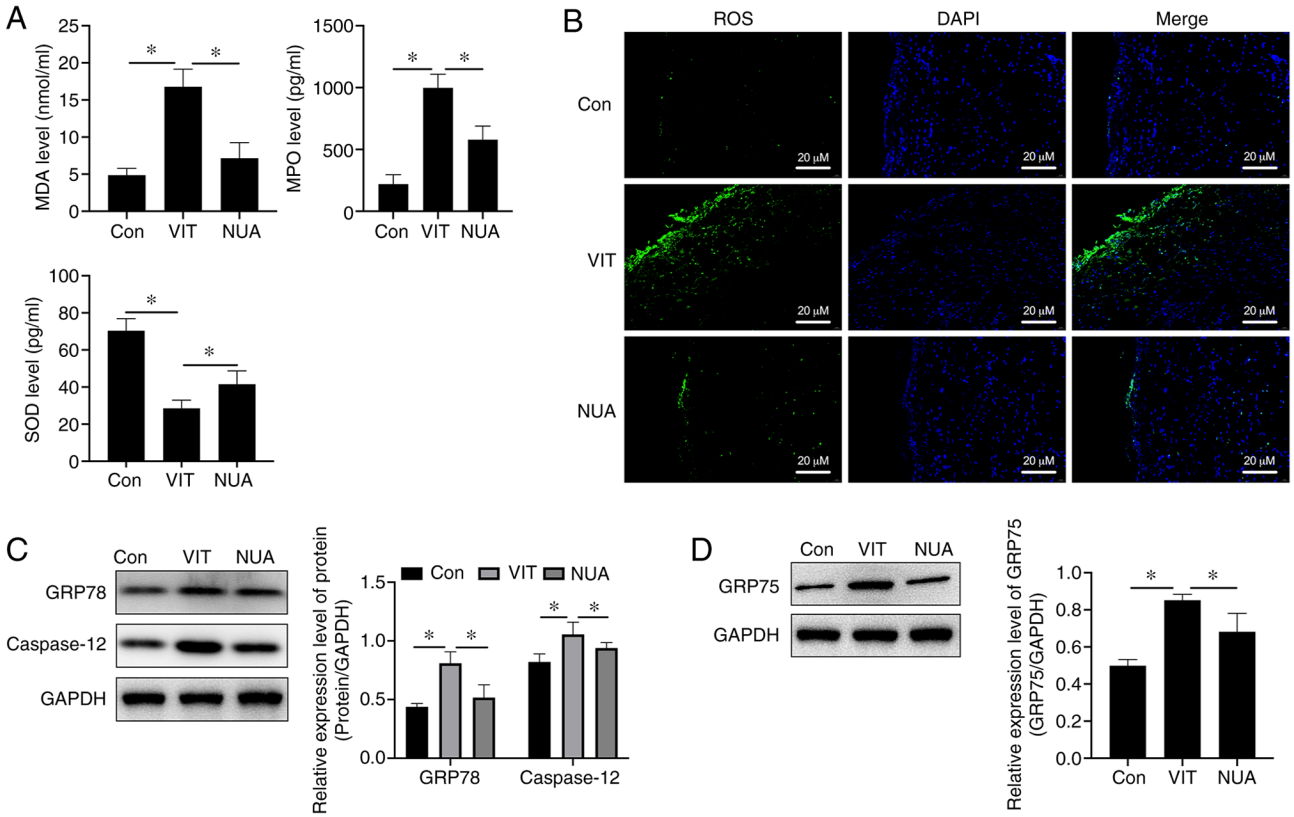

Figure 3. ER stress homeostasis regulated by NB-UVB/ADSCs transplantation treatment. (A) Oxidative stress level detected by ELISA. (B) ROS detected by immunofluorescence (scale bar=20 μm). (C) The relative expression level of protein (GRP78 and caspase-12) detected by western blotting. (D) GRP75 expression level detected by western blotting. All the data are represented as the mean ± standard deviation (n=3). *P<0.05. ER, endoplasmic reticulum; NB-UVB, narrow band ultraviolet B; ADSCs, adipose-derived stem cells; ROS, reactive oxygen species; GRP, glucose-regulated protein; Con, mice were treated with Vaseline only; VIT, mice in vitiligo model group treated with 40% monobenzone cream; NUA, mice treated with narrow band ultraviolet B and adipose-derived stem cells together.

successfully established. Additionally, MBZ may also trigger autoimmunity to melanocytes by causing T cell differentiation. These findings are in accordance with vitiligo progression in humans (25).

Ca^{2+} homeostasis has been implicated in various cellular functions such as myofilament contraction, hormone secretion and metabolism modulation (26). It also has a critical role in triggering cell death (27). The ER is the intracellular Ca^{2+} storage reservoir in mammals (28). Under ER stress, Ca^{2+} is released from the ER into the cytosol through either IP3R receptors or (RyR receptors, resulting in the activation of mitochondria (29). In this process, VDAC, a mitochondrial Ca^{2+} transporter and IP3R are coupled by GRP75, followed by the activation of other mitochondrial Ca^{2+} transporters such as MCUR (30). The present study found upregulation of Ca^{2+} transporters, including IP3R, RYR1, VDAC2 and MCUR1 and of GRP75 in vitiligo mice, which supported the notion that the ER and mitochondria contact and crosstalk via Ca^{2+}. These activations of Ca^{2+} transporters were attenuated by NB-UVB irradiation in ADSCs-transplanted mice, suggesting the treatment of vitiligo mice with NB-UVB/ADSCs transplantation combined therapy works via regulating cellular Ca^{2+} homeostasis.

Since the major function of the SERCA2 pump is to transport Ca^{2+} from the cytosol into the ER, MBZ-mediated downregulation of SERCA2 possibly induced an alteration of cellular Ca^{2+} homeostasis. In Biagioli *et al* (31), disruption of ER Ca^{2+} homeostasis compromises the ER compartment, leading to ER stress and caspase-12-dependent apoptosis. These events were also found in the present study, which found that NB-UVB/ADSCs transplantation combined therapy improved expression of both SERCA2 and caspase-12, indicating that it affected caspase-12-dependent cell apoptosis.

Ca^{2+} overload also stimulates ROS accumulation (32). It has been reported that either generation of ROS or compromised antioxidant activity contributes to vitiligo (33). The data of the present study suggested a loss of redox balance in MBZ-treated mice as illustrated in Fig. 2B. The Nrf2/HO-1 antioxidant system is known to be functionally deficient in patients with vitiligo (34). Consistent with this fact, the present study observed inhibition of Nrf2 by MBZ treatment, accompanied by downregulation of HO-1 and thioredoxin-1 (Fig. 5A), with these inhibitions restored in NB-UVP/ADSCs transplantation treated mice. These data suggested a weakened Nrf2/HO-1 antioxidant system in vitiligo mice that was repaired by the combination therapy. The protective effect of the combined therapy on vitiligo was abolished by the Nrf2 inhibitor. Considering these data together, treatment of vitiligo by NB-UVB/ADSCs transplantation combined therapy is mediated by Nrf2/HO-1 signaling.

In conclusion, the present study demonstrated for the first time that NB-UVB/ADSCs transplantation combined

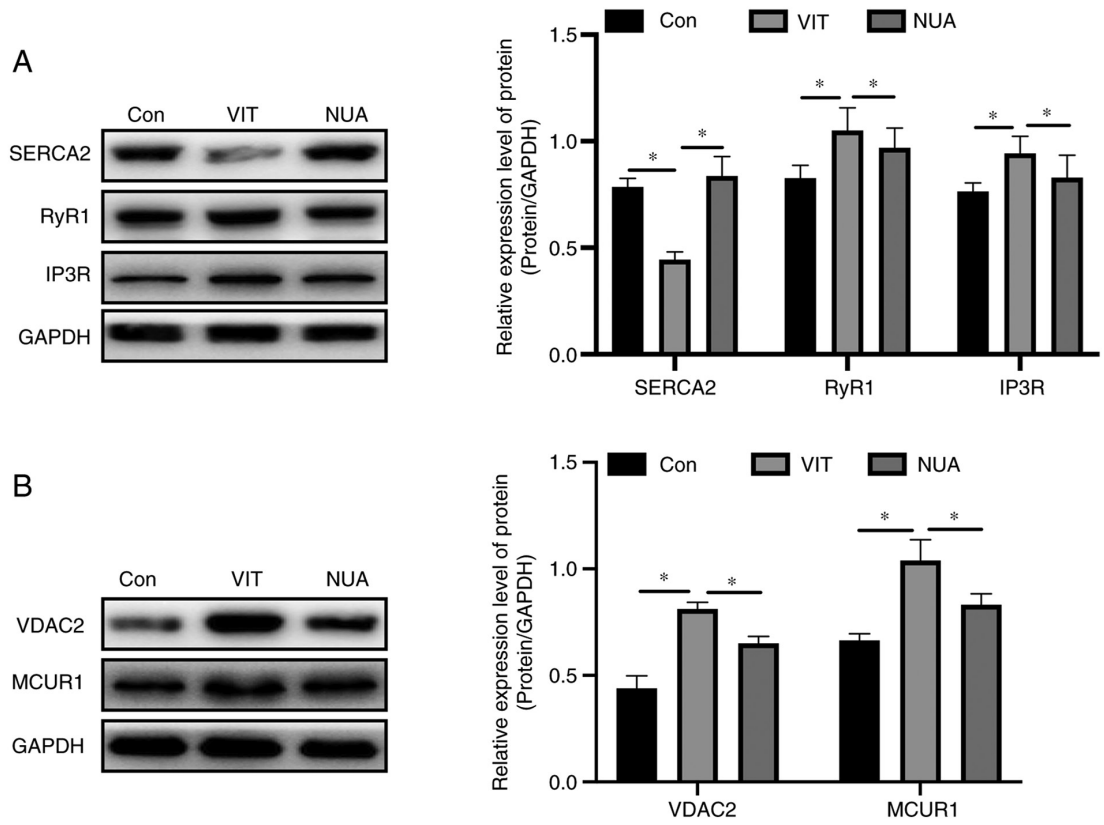

Figure 4. The effect of NB-UVB/ADSCs transplantation treatment on ER stress and Ca^{2+} homeostasis. The ER stress-associated (A) proteins and (B) Ca^{2+} channels were analyzed by western blotting, respectively. The data are represented as the mean ± standard deviation (n=3). *P<0.05. NB-UVB, narrow band ultraviolet B; ADSCs, adipose-derived stem cells; ER, endoplasmic reticulum; RYR1, ryanodine receptor; IP3R, inositol 1,4,5-trisphosphate receptor; Con, mice were treated with Vaseline only; VIT, mice in vitiligo model group treated with 40% monobenzone cream; NUA, mice treated with narrow band ultraviolet B and adipose-derived stem cells together.

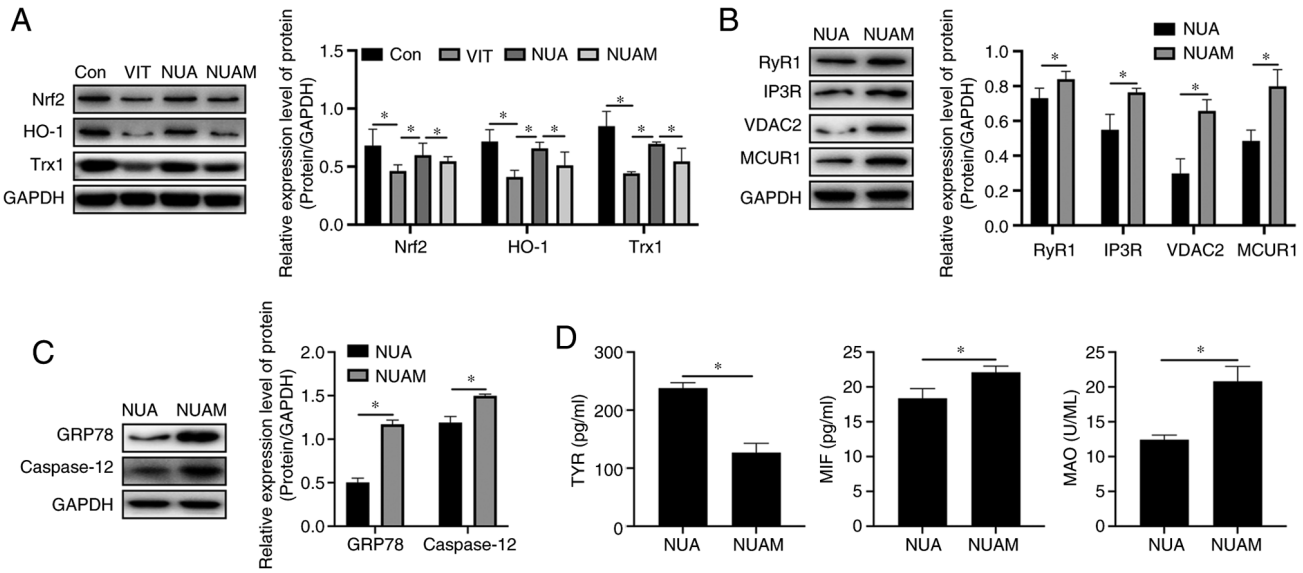

Figure 5. Treatment of vitiligo by NB-UVB is mediated by Nrf2/HO-1 signaling. The (A) Nrf2/HO-1 signaling and (B) expression of Ca^{2+} channels was examined by western blotting. (C) ER stress-related proteins levels detected by western blotting. (D) The levels of diagnostic markers of vitiligo were measured by ELISA. All the data are represented as the mean ± standard deviation (n=3). *P<0.05. NB-UVB, narrow band ultraviolet B; Nrf2, nuclear factor erythroid 2 like 2; HO-1, heme oxygenase 1; Trx-1, thioredoxin-1; Con, mice were treated with Vaseline only; VIT, mice in vitiligo model group treated with 40% monobenzone cream; NUA, mice treated with narrow band ultraviolet B and adipose-derived stem cells together; NUAM, vitiligo model treated with NB-UVB/ADSCs and Nrf2 inhibitor ML385.

therapy improved MBZ-induced vitiligo in mice. Probable mechanisms for this protection are inhibition of ER stress and regulation of ER Ca^{2+} homeostasis through Nrf2/HO-1 signaling. These findings improve our understanding of the

pathogenesis of vitiligo and will guide future development of therapeutic strategies against vitiligo.

Acknowledgements

Not applicable.

Funding

The present study was supported by Liaoning Province Immunological Skin Disease Diagnosis and Treatment Technical Specification Laboratory (grant no. 111/2400017006) and Key Research and Development Program of Liaoning Province (grant no. 2018225058).

Availability of data and materials

The datasets used and/or analyzed during the current study are available from the corresponding author on reasonable request.

Authors' contributions

YB and HY performed the whole experiment and confirm the authenticity of all the raw data. MJ analyzed and interpreted data analyisis. YB and XG contributed to the study design and drafted the manuscript. All authors read and approved the final version of manuscript.

Ethics approval and consent to participate

All procedures were performed according to Center for Animal Resources and Development regulations for animal care and approved by Institutional Animal Care and Use Committee of CMU (approval no. CMU2019211).

Patient consent for publication

Not applicable.

Competing interests

The authors declare that they have no competing interests.

References

1. Ezzedine K, Eleftheriadou V, Whitton M and van Geel N: Vitiligo. Lancet 386: 74-84, 2015.
2. Ezzedine K, Lim HW, Suzuki T, Katayama I, Hamzavi I, Lan CC, Goh BK, Anbar T, Silva de Castro C, Lee AY, *et al*: Revised classification/nomenclature of vitiligo and related issues: The Vitiligo Global Issues Consensus Conference. Pigment Cell Melanoma Res 25: E1-E13, 2012.
3. Elbuluk N and Ezzedine K: Quality of life, burden of disease, co-morbidities, and systemic effects in vitiligo patients. Dermatol Clin 35: 117-128, 2017.
4. Manga P, Elbuluk N and Orlow SJ: Recent advances in understanding vitiligo. F1000Research 5, 2016.
5. Denman CJ, McCracken J, Hariharan V, Klarquist J, Oyarbide-Valencia K, Guevara-Patiño JA and Le Poole IC: HSP70i accelerates depigmentation in a mouse model of autoimmune vitiligo. J Invest Dermatol 128: 2041-2048, 2008.
6. Yildirim M, Korkmaz S and Erturan İ: Role of antioxidants in vitiligo. Comprehensive Textbook on Vitiligo: 145, 2020.
7. Eletto D, Chevet E, Argon Y and Appenzeller-Herzog C: Redox controls UPR to control redox. J Cell Sci 127: 3649-3658, 2014.
8. Krebs J, Groenendyk J and Michalak M: Ca2+-signaling, alternative splicing and endoplasmic reticulum stress responses. Neurochem Res 36: 1198-1211, 2011.
9. Xiao BH, Wu Y, Sun Y, Chen HD and Gao XH: Treatment of vitiligo with NB-UVB: A systematic review. J Dermatolog Treat 26: 340-346, 2015.
10. Njoo M, Bos J and Westerhof W: Treatment of generalized vitiligo in children with narrow-band (TL-01) UVB radiation therapy. J Am Acad Dermatol 42: 245-253, 2000.
11. Karaosmanoglu N, Ozdemir Cetinkaya P, Kutlu O, Karaaslan E, Imren IG, Kiratli Nalbant E and Eksioglu M: A cross-sectional analysis of skin cancer risk in patients receiving narrow-band ultraviolet B phototherapy: An evaluation of 100 patients. Arch Dermatol Res 312: 249-253, 2020.
12. Buglewicz DJ, Mussallem JT, Haskins AH, Su C, Maeda J and Kato TA: Cytotoxicity and mutagenicity of narrowband UVB to mammalian cells. Genes (Basel) 11: 646, 2020.
13. Si Z, Wang X, Sun C, Kang Y, Xu J, Wang X and Hui Y: Adipose-derived stem cells: Sources, potency, and implications for regenerative therapies. Biomed Pharmacother 114: 108765, 2019.
14. Bajek A, Gurtowska N, Olkowska J, Kazmierski L, Maj M and Drewa T: Adipose-derived stem cells as a tool in cell-based therapies. Arch Immunol Ther Exp (Warsz) 64: 443-454, 2016.
15. Rigotti G, Marchi A, Galiè M, Baroni G, Benati D, Krampera M, Pasini A and Sbarbati A: Clinical treatment of radiotherapy tissue damage by lipoaspirate transplant: A healing process mediated by adipose-derived adult stem cells. Plast Reconstr Surg 119: 1409-1422, 2007.
16. Sándor GK, Tuovinen VJ, Wolff J, Patrikoski M, Jokinen J, Nieminen E, Mannerström B, Lappalainen OP, Seppänen R and Miettinen S: Adipose stem cell tissue-engineered construct used to treat large anterior mandibular defect: A case report and review of the clinical application of good manufacturing practice-level adipose stem cells for bone regeneration. J Oral Maxillofac Surg 71: 938-950, 2013.
17. Lim WS, Kim CH, Kim JY, Do BR, Kim EJ and Lee AY: Adipose-derived stem cells improve efficacy of melanocyte transplantation in animal skin. Biomol Ther (Seoul) 22: 328, 2014.
18. Mukhatayev Z, Dellacecca ER, Cosgrove C, Shivde R, Jaishankar D, Pontarolo-Maag K, Eby JM, Henning SW, Ostapchuk YO, Cedercreutz K, *et al*: Antigen specificity enhances disease control by Tregs in vitiligo. Front Immunol 11: 581433, 2020.
19. Zhao Y, Wang N, Wu H, Zhou Y, Huang C, Luo J, Zeng Z and Kong L: Structure-based tailoring of the first coumarins-specific bergaptol O-methyltransferase to synthesize bergapten for depigmentation disorder treatment. J Adv Res 21: 57-64, 2020.
20. Chen J, Tang YX, Liu YM, Chen J, Hu XQ, Liu N, Wang SX, Zhang Y, Zeng WG, Ni HJ, *et al*: Transplantation of adipose-derived stem cells is associated with neural differentiation and functional improvement in a rat model of intracerebral hemorrhage. CNS Neurosci Ther 18: 847-854, 2012.
21. Lv W, Graves DT, He L, Shi Y, Deng X, Zhao Y, Dong X, Ren Y, Liu X, Xiao E and Zhang Y: Depletion of the diabetic gut microbiota resistance enhances stem cells therapy in type 1 diabetes mellitus. Theranostics 10: 6500-6516, 2020.
22. Singh A, Venkannagari S, Oh KH, Zhang YQ, Rohde JM, Liu L, Nimmagadda S, Sudini K, Brimacombe KR, Gajghate S, *et al*: Small molecule inhibitor of NRF2 selectively intervenes therapeutic resistance in KEAP1-deficient NSCLC tumors. ACS Chem Biol 11: 3214-3225, 2016.
23. Liu X, Zhu Q, Zhang M, Yin T, Xu R, Xiao W, Wu J, Deng B, Gao X, Gong W, *et al*: Isoliquiritigenin ameliorates acute pancreatitis in mice via inhibition of oxidative stress and modulation of the Nrf2/HO-1 pathway. Oxid Med Cell Longev 2018: 7161592-7161592, 2018.
24. Dicle O: Assessment methods in vitiligo. Pigment Disord 2: 1, 2015.
25. Zhu Y, Wang S and Xu A: A mouse model of vitiligo induced by monobenzone. Exp Dermatol 22: 499-501, 2013.
26. Pinton P, Giorgi C, Siviero R, Zecchini E and Rizzuto R: Calcium and apoptosis: ER-mitochondria Ca2+ transfer in the control of apoptosis. Oncogene 27: 6407-6418, 2008.
27. Giorgi C, Romagnoli A, Pinton P and Rizzuto R: Ca2+ signaling, mitochondria and cell death. Curr Mol Med 8: 119-130, 2008.
28. Carreras-Sureda A, Pihán P and Hetz C: Calcium signaling at the endoplasmic reticulum: Fine-tuning stress responses. Cell Calcium 70: 24-31, 2018.

29. Buckley C, Wilson C and McCarron JG: FK506 regulates Ca^{2+} release evoked by inositol 1,4,5-trisphosphate independently of FK-binding protein in endothelial cells. Br J Pharmacol 177: 1131-1149, 2020.
30. De Brito OM and Scorrano L: An intimate liaison: Spatial organization of the endoplasmic reticulum-mitochondria relationship. EMBO J 29: 2715-2723, 2010.
31. Biagioli M, Pifferi S, Ragghianti M, Bucci S, Rizzuto R and Pinton P: Endoplasmic reticulum stress and alteration in calcium homeostasis are involved in cadmium-induced apoptosis. Cell Calcium 43: 184-195, 2008.
32. Rimessi A, Previati M, Nigro F, Wieckowski MR and Pinton P: Mitochondrial reactive oxygen species and inflammation: Molecular mechanisms, diseases and promising therapies. Int J Biochem Cell Biol 81: 281-293, 2016.
33. Denat L, Kadekaro AL, Marrot L, Leachman SA and Abdel-Malek ZA: Melanocytes as instigators and victims of oxidative stress. J Invest Dermatol 134: 1512-1518, 2014.
34. Jian Z, Li K, Song P, Zhu G, Zhu L, Cui T, Liu B, Tang L, Wang X, Wang G, *et al*: Impaired activation of the Nrf2-ARE signaling pathway undermines H2O2-induced oxidative stress response: A possible mechanism for melanocyte degeneration in vitiligo. J Invest Dermatol 134: 2221-2230, 2014.